Ab initio study of native point-defects in $CoSb_3$: Understanding off-stoichiometric doping properties

Chan-Hyun Park and Yong-Sung Kim*
Korea Research Institute of Standards and Science, P.O. Box 102, Yuseong, Daejeon 305-600, Korea
(Received 7 October 2009; revised manuscript received 30 November 2009; published 8 February 2010)

Undoped Co-rich $CoSb_3$ is known to be *n*-type at room temperature and changed into *p*-type at high temperature above about 500 K, while undoped Sb-rich $CoSb_3$ is *p*-type independently of temperature. Based on *ab initio* calculations, it is found that Co-interstitial-pairs cause the *n*-type doping in Co-rich $CoSb_3$. Above the pair decomposition temperature, which depends on the Sb deficiency, isolated Co interstitials can lead to the *p*-type doping. Co vacancies are found to dominate the *p*-type doping in Sb-rich $CoSb_3$.

DOI: 10.1103/PhysRevB.81.085206 PACS number(s): 61.72.Bb, 71.55.Ht

I. INTRODUCTION

$CoSb_3$ skutterudite compounds have attracted great attention for the promising application in a good thermoelectric material.[1–4] In growth of $CoSb_3$, a nonstoichiometric condition is easily encountered.[5,6] The $CoSb_3$ grown with undoped has either *n*-type[5–10] or *p*-type[5,9–14] conductivity. The different types of $CoSb_3$ have been tentatively considered to be related to a slight deviation from the stoichiometric ratio of $CoSb_3$.[5,6,9,10]

The Sb/Co ratio can be controlled by the volatilization of Sb, which can occur at high temperature during the growth process[5,9,10] and/or incorporation of excess Sb.[10] The detailed studies on the nonstoichiometric $CoSb_3$ have found puzzling dependences of the carrier types on the Sb/Co ratio and the measurement temperature of Seebeek coefficient. In Sb-rich $CoSb_3$, a positive Seebeek coefficient (*p*-type) has been found and a negative value (*n*-type) has been measured in Co-rich $CoSb_3$ at room temperature.[5,9,10] While the *p*-type in Sb-rich $CoSb_3$ is preserved as increasing the temperature, the *n*-type in Co-rich $CoSb_3$ has been found to be changed into *p*-type at high temperature above about 500 K.[5,7–10]

The knowledge of the governing native point-defects and their electrical properties, such as defect levels, are essential to understand the electrical properties of nonstoichiometric $CoSb_3$. Although the bulk electronic structure[8,15–18] and thermoelectric properties[4] have been studied extensively by using density-functional theory calculations, there has been lack of comprehensive theoretical studies on the native point-defects in $CoSb_3$. In Ref. 8, Sb vacancies (V_{Sb}) and Sb-interstitials (Sb_i) were considered for the nonstoichiometric native point-defects without detailed discussions on the stabilities. Due to the easy volatility of Sb, V_{Sb} has been treated as an important native point defect in Co-rich $CoSb_3$.[8–10] However, in this study, we show that Co vacancies (V_{Co}) and Co interstitials (Co_i) are significant of playing key roles in determining the off-stoichiometric doping properties in $CoSb_3$. We find that V_{Co} and Co_i are the dominant *p*-type sources in Sb-rich and Co-rich $CoSb_3$, respectively, and Co_i-pairs can cause the *n*-type doping in Co-rich $CoSb_3$. The decomposition temperature of the Co_i-pairs corresponds to the transition temperature of the majority carrier types in Co-rich $CoSb_3$, which is estimated to be about 420–600 K depending on the Sb deficiency with the Co_i concentrations of an order of 10^{19} cm^{-3}. The stabilities and the detailed atomic and electronic structures of the native point-defects in $CoSb_3$ are discussed.

II. METHODS

We performed density-functional theory calculations as implemented in the Vienna *ab initio* simulation package code.[19] The projector-augmented wave pseudopotentials[20] and the local density approximation (LDA) for the exchange correlation energy[21] were used. A kinetic energy cutoff of 300 eV, 256-atomic cubic supercell, and the Γ point for the *k*-point sampling were used. The Hellmann-Feynman forces were relaxed until less than 0.01 eV/Å.

The calculated bulk properties of $CoSb_3$ are summarized in Table I, compared with the other calculations and experiments. The calculated lattice and internal parameters are $a=8.917$ Å, $u=0.333$, and $v=0.155$. They are close to the other LDA calculation.[16] The calculated lattice constant, *a*, is slightly lower than the experimental value of $a=9.0385$ Å.[22] The theoretical value of $a=8.917$ Å was used in our defect calculations.

The calculated LDA band gap is 0.26 eV, which is close to the other LDA calculation, 0.22 eV,[16] and higher than the generalized-gradient approximation (GGA) calculations, 0.17 and 0.118 eV.[16,17] The calculated gap is smaller than the experimental gap of about 0.5 eV.[14,23] In spite of the gap underestimation, the LDA can give essential information on defect systems in various semiconductors.[24,25] No gap correction was applied in this study.

Only the crystalline skutterudite structure was considered for the defect host, not a disordered system. Experimentally, single crystalline[11,12,14,26] and poly-crystalline[5–10,13] $CoSb_3$ samples have been studied. By the large 256-atomic supercell ($Co_{64}Sb_{192}$), the presence of a single native point defect in the supercell yields the defect concentrations of 1.56% for V_{Co} and Co_i and 0.52% for V_{Sb} and Sb_i. The interactions between supercells are found to be weak and the energy convergence with respect to the supercell size is achieved within the accuracy of less than 200 meV, as will be discussed in Sec. III B.

III. RESULTS

A. Atomic structures

We first investigate the atomic structure of Co_i. We find six different Co_i structures and the most stable one is shown

TABLE I. Comparison between experimental and theoretical results for the lattice (a), internal parameters (u and v), and band gap (E_g) of $CoSb_3$.

Reference	Method	a (Å)	u	v	E_g (eV)
Our calc.	LDA	8.917	0.333	0.155	0.26
Ref. 16	LDA	8.94	0.3328	0.1599	0.22
Ref. 16	GGA	9.14	0.3332	0.1594	0.17
Ref. 17	GGA	9.144	0.3330	0.1592	0.118
Ref. 22	Expt.	9.0385	0.33537	0.15788	
Ref. 14	Expt.				0.55
Ref. 23	Expt.				0.5

in Fig. 1(a). The Co_i is located between 3 Sb_4 pnictide rings, and has the coordination number of seven consisted of 5 Co_i-Sb and 2 Co_i-Co bonds (sevenfold Co_i). We find the energy of Co_i is well correlated with the coordination number of Co_i. At the void center, where there is no Sb_4 pnictide ring in the skutterudite $CoSb_3$ [Fig. 1(f)], the Co_i has no bond and is 2.41 eV higher in energy. On the plane of a pnictide ring, the coordination number of Co_i is four [Figs. 1(d) and 1(e)], and it is 1.16–1.59 eV higher in energy. When the Co_i has the coordination numbers of five [Fig. 1(c)] and six [Fig. 1(b)] (sixfold Co_i) separately, the energies are found to be higher by 0.57 and 0.43 eV, respectively. We could not find an interstitial site, where the Co_i has more than seven coordination number, and the sevenfold Co_i structure is thought to be the most stable one in the skutterudite $CoSb_3$. The relative stabilities are for the neutral charge state and similar for the charged states of Co_i.

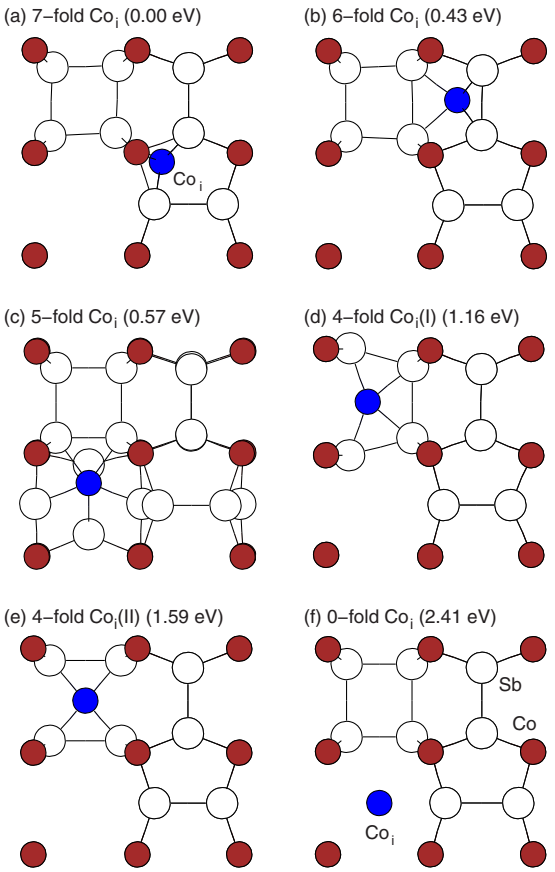

FIG. 1. (Color online). Relaxed atomic structures of various Co_i structures. The small and large circles are Co and Sb atoms, respectively. The interstitial atoms are indicated by the blue (dark gray) color. The energies relative to the most stable sevenfold Co_i are indicated.

For Sb_i, two different atomic structures are found [Figs. 2(a) and 2(b)]. Figure 2(a) shows the most stable void-center Sb_i configuration. When Sb_i is located at the Sb_4 ring-center site, it is 2.38 eV higher in energy. The large energy difference in the neutral charge state is also found for the charged states of Sb_i.

The eight Co atoms in the skutterudite $CoSb_3$ conventional cell are all equivalent, and there is only one possible inequivalent atomic site for the V_{Co}. The relaxed atomic structure of V_{Co} is shown in Fig. 2(c). In the V_{Co} structure,

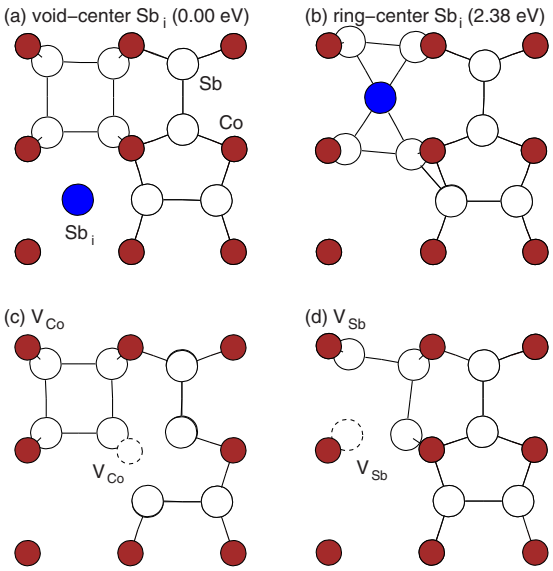

FIG. 2. (Color online). Relaxed atomic structures of (a) void-center Sb_i, (b) ring-center Sb_i, (c) V_{Co}, and (d) V_{Sb}. The small and large circles are Co and Sb atoms, respectively. The interstitial atoms are indicated by the blue (dark gray) color. The dashed circles indicate the vacancy sites. For Sb_i, the energies relative to the most stable void-center Sb_i are indicated.

there is no large lattice distortion, but slight changes in the nearby Sb_4 bond lengths are found. In the ideal skutterudite $CoSb_3$, the long Sb-Sb bond length of Sb_4 is 2.984 Å, and the short one is 2.864 Å in our calculations. In the V_{Co} structure in the neutral charge state, the long bond near the V_{Co} is increased by about 0.5% (2.997 Å), and the short bond by about 1% (2.882 Å).

The 24 Sb atoms in the $CoSb_3$ conventional cell are all equivalent by symmetry and there is only one possible inequivalent atomic site for the V_{Sb}. The relaxed atomic structure of V_{Sb} is shown in Fig. 2(d). The Sb_4 pnictide ring is broken by the single V_{Sb} and the Sb_3 broken ring is distorted with accompanying a large lattice relaxation. The two Sb-Sb bond lengths of the Sb_3 in the neutral charge state are 2.830 and 3.036 Å, which are shorter by 1.2% and longer by 1.7% than the short and long bonds of the Sb_4 in $CoSb_3$, respectively. The Sb_3 broken ring is rotated by about 6° from the original position of Sb_4, and the ∠Sb-Sb-Sb bond angle is calculated to be 93.8°.

B. Formation energies

In order to compare the stabilities between the native point-defects in various charged states under off-stoichiometric condition, we calculated the formation energy (E_f) of a defect as a function of Co (μ_{Co}), Sb (μ_{Sb}), and electronic (μ_e) chemical potentials, which is defined as the following:

$$E_f = E_t - n_{Co}\mu_{Co} - n_{Sb}\mu_{Sb} + q\mu_e, \quad (1)$$

where E_t is the total energy of the supercell containing a defect, n_{Co} and n_{Sb} are the number of Co and Sb atoms in the supercell, and q is the charge of the defect. The formation energy of $CoSb_3$ bulk is referenced to $E_f=0$ by the condition of $\mu_{Co}+3\mu_{Sb}=E_t(CoSb_3)$. The total energy of a pure Co hcp metal is chosen for the μ_{Co} in the Co-rich limit, and the total energy of a pure Sb rhombohedral metal for the μ_{Sb} in the Sb-rich limit. The calculated heat of formation of $CoSb_3$ with respect to the Co and Sb metals is −1.39 eV/$CoSb_3$, which is close to the experimental value of −1.276 eV/$CoSb_3$ (−123.158 kJ/mol) for the sample grown at 1000 K.[27] Between the Co-rich and Sb-rich limit, the $CoSb_3$ bulk is stable with respect to the Co and Sb metals, and the pure Co and Sb metal formation is prevented. The electronic chemical potential, μ_e, can be written as $\mu_e=\varepsilon_f+E_v$, where ε_f is the Fermi level with respect to the valence-band maximum (VBM) energy, E_v. The determination of the E_v of the defect-containing $CoSb_3$ supercell is done by $E_v=E_v^{CoSb_3}+\Delta E_v$, where $E_v^{CoSb_3}$ is the VBM energy of $CoSb_3$ bulk, and ΔE_v is the electrostatic energy shift between the bulk and the defect-containing supercells. The detailed calculation method of the defect formation energy is described in many literatures.[28–31]

For the most stable configurations of the native point-defects shown in Sec. III A, the calculated formation energies as a function of the Fermi level, ε_f, are drawn in Fig. 3. In the Co-rich limit, the Co_i is found to be exceptionally low in formation energy. It is about 0.80 eV in the neutral charge state, while those of Sb_i, V_{Co}, and V_{Sb} are over 2.0 eV. Thus, the Co_i is expected to be the dominant native point defect in

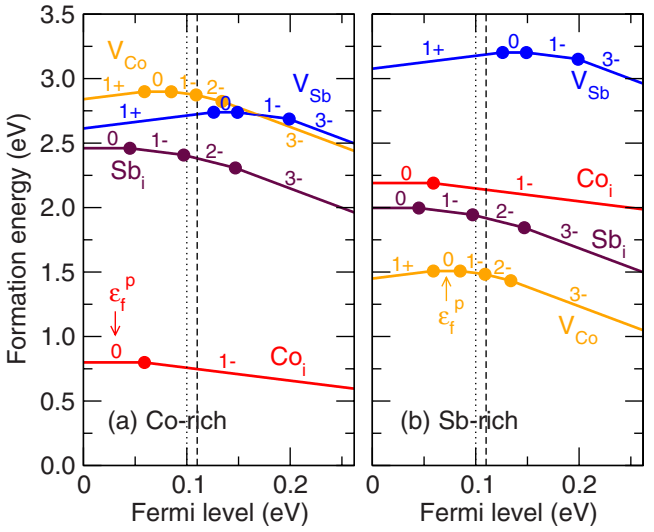

FIG. 3. (Color online). Calculated formation energies of Co_i, Sb_i, V_{Co}, and V_{Sb} plotted as a function of the Fermi level in the (a) Co-rich and (b) Sb-rich limit of $CoSb_3$. The dashed and dotted lines indicate the intrinsic Fermi levels at room temperature and 600 K, respectively. The pinning level by the dominant defects is indicated by ε_f^p.

Co-rich $CoSb_3$. In Sb-rich $CoSb_3$, the V_{Co} is found to be the dominant. The formation energy is about 1.5 eV in the neutral charge state. The V_{Sb} is found to be very high in formation energy both in Co-rich and Sb-rich $CoSb_3$. The breaking of the strong covalent Sb_4 pnictide ring bonds [Fig. 2(d)] is considered to require high energies. Although V_{Sb} has been thought to be an important defect with the typical Sb-deficiency in $CoSb_3$,[8–10] its concentration is not expected to be high.

Since the calculations on the defect-containing supercells can give spurious electrostatic interactions between supercells, we checked the formation energy changes by the Makov and Payne correction scheme.[32] For V_{Co} in the (1−), (2−), and (3−) charged states [same in the (1+), (2+), and (3+) charged states], the monopole correction leads to the increases in the formation energies by 0.034, 0.137, and 0.308 eV, respectively. The dipole and quadrupole corrections yield the changes of −0.012, −0.048, and −0.108 eV for the (1−), (2−), and (3−) charged states, and −0.010, −0.041, and −0.092 eV for the (1+), (2+), and (3+) charged states, respectively. Thus, the total corrections including the monopole, dipole, and quadrupole interactions are only 0.022, 0.088, and 0.200 eV for the (1−), (2−), and (3−) charged states, and similarly 0.024, 0.096, and 0.216 eV for the (1+), (2+), and (3+) charged states, respectively. The total energy corrections are only a few tens of meV up to the doubly charged states and about 200 meV for the triply charged states. These values do not significantly affect the formation energies of the native point-defects shown in Fig. 3, and do not change the main results without the corrections. It is basically due to the high dielectric constant of 33.5 in $CoSb_3$ (Refs. 12, 18, and 33) and the large supercell containing 256 atoms. Thus, the spurious electrostatic interactions between supercells are considered to be small in our calculations.

We also checked the formation energies of V_{Co} in difference supercell sizes. The formation energy of V_{Co} in the (0), (1−), (2−), and (3−) states are 1.508, 1.603, 1.722, and 1.866 eV in the Sb-rich limit in the 256-atomic supercell, respectively, when the ε_f is at the VBM. They are, in 32-atomic supercell, 1.674, 1.628, 1.644, and 1.721 eV, respectively. The differences are only −166, −25, 78, and 145 meV, respectively, and thus the convergence of the formation energies with respect to the supercell size is considered to be achieved within less than 200 meV in our 256-atomic supercell calculations.

C. Electronic structures

From the defect formation energies as a function of the ε_f in the band gap shown in Fig. 3, we can see the electrical properties, such as transition levels, of the defects. The preferred charge state of a defect can be identified by comparing the formation energies between difference charge states. At the cross points of the formation energies of a defect between difference charge states indicate the transition levels, which are seen as kinks in the formation energy lines (we put dots at the kinks for clarity) in Fig. 3. When ε_f is near the VBM, if the defect prefers to be negatively charged, it is an acceptorlike defect generating a hole in the VBM, while when ε_f is near the conduction-band minimum (CBM), if the defect to be positively charged, it is a donorlike defect easily giving a free electron to the CBM. We can also find the equilibrium Fermi level under the dominant presence of a defect. For example, in the dominant presence of acceptors (negatively charged defects), the equilibrium Fermi level becomes located near the VBM, while in the dominant presence of donors (positively charged defects), the equilibrium Fermi level lies near the CBM.

In Co-rich $CoSb_3$, the Co_i is the dominant native point defect species. The Co_i is found to be an acceptorlike defect. The calculated (0/1−) acceptor level lies at E_v+58 meV (Fig. 3). The number of valence electrons of a Co atom is nine. The fully occupied four 3*d*-like states of Co_i are found inside the valence bands, and the singly occupied topmost 3*d*-like state is found just above the VBM, as shown in the calculated projected local density of states in Fig. 4(a). The singly occupied 3*d*-like state in the gap acts as the acceptor state, making the Co_i be a shallow single acceptor in $CoSb_3$. By the bonding of Co_i with the surrounding 7 Co and Sb atoms [Fig. 1(a)], the 3*d*-like states are stabilized with lowering their levels, by which the two 4*s* electrons are intra-atomically transferred into the 3*d*-like states. The single 4*s*-like state of Co_i is found to be delocalized inside the conduction bands.

In a narrow gap semiconductor, the intrinsic carrier concentrations can be significant even at room temperature. The $CoSb_3$ has a high electronic density of states near the CBM, as compared to that near the VBM.[15–17] Thus, the intrinsic (without defects) Fermi level (ε_f^0) is located at the lower part of the band gap. The calculated ε_f^0 is E_v+0.11 eV at room temperature, indicated in Fig. 3, and E_v+0.10 eV at 600 K. The Co_i (0/1−) transition level and the corresponding pinning Fermi level (ε_f^p) by the dominant presence of Co_i's are found to be lower than the ε_f^0 [Fig. 3(a)], resulting in a higher concentration of holes as a majority carrier and thus *p*-type in Co-rich $CoSb_3$.

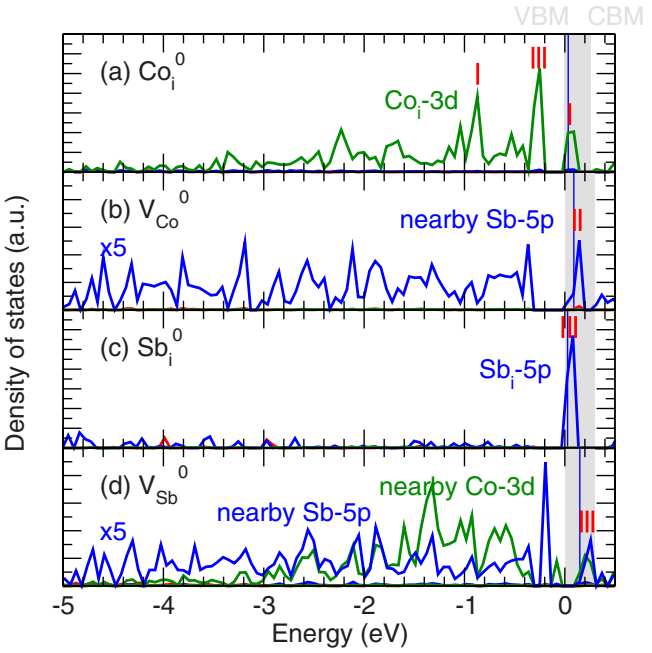

FIG. 4. (Color online). Projected local electronic densities of states of (a) Co_i, (b) V_{Co}, (c) Sb_i, and (d) V_{Sb} in the neutral charge states. Gap is shown by the gray shade. The defect levels are schematically indicated by the short thick vertical bars near the peaks. The thin vertical lines in the gap indicate the highest singly occupied level.

The V_{Co} can act as a shallow acceptor. The calculated (0/1−) transition level lies at E_v+85 meV (Fig. 3). The V_{Co} can be charged up to (3−), and the calculated (1−/2−) and (2−/3−) transition levels are E_v+109 and 134 meV, respectively. The Co cation and Sb anion in $CoSb_3$ have the formal oxidation states of the Co^{3+} and Sb_4^{4-}. By the V_{Co} formation, i.e., by the absence of a Co atom, three electrons are lack in $CoSb_3$, and thus three holes are generated in the Sb_4-related valence bands. The highest occupied state of an Sb_4 molecular species is known as π_4.[34] There are 6 Sb_4 rings adjacent to a V_{Co}, and thus the 6 π_4-like states of the 6 Sb_4 become the defect-related states of V_{Co}. The emerged defect states into the gap induced by the π_4 are found to be two and slightly above the VBM [see Figs. 4(b) and 5], and thus the V_{Co} is a shallow triple acceptor. A single electron can be

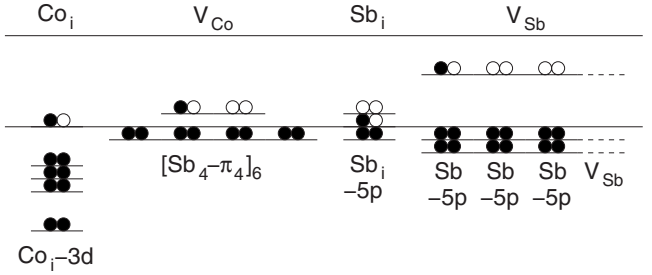

FIG. 5. Schematic figure of the defect-related states of Co_i, V_{Co}, Sb_i, and V_{Sb} in the neutral charge state.

released from the V_{Co} (V_{Co}^{1+}), when the Fermi level is very low below E_v+58 meV (Fig. 3), i.e., the V_{Co} can also act as a hole trap. In the dominant presence of V_{Co} in Sb-rich $CoSb_3$, the ε_f is thus pinned slightly above the VBM, as indicated by an arrow in Fig. 3(b). The pinning level, ε_f^p, is found to be lower than the intrinsic Fermi level, ε_f^0, of $CoSb_3$, and thus the dominant presence of V_{Co} can lead to a higher concentration of holes and *p*-type in Sb-rich $CoSb_3$.

For completeness, we shortly discuss the electronic structures of Sb_i and V_{Sb}, even though they are high in formation energy. The Sb_i is found to be a shallow triple acceptor. The calculated (0/1−), (1−/2−), and (2−/3−) levels are E_v+44, 96, and 146 meV, respectively (Fig. 3). The topmost valence state of an Sb atom is triply degenerated 5*p*. At the void-center site, the Sb_i has a cubic symmetry and the level degeneracy is conserved. The defect state of Sb_i is found to be 5*p*-like occupied by three electrons, of which levels are slightly above the VBM [see Figs. 4(c) and 5], and thus the Sb_i is a shallow triple acceptor.

The defect state of V_{Sb} is related to the Sb-5*p* states of the Sb_3 broken ring. The Sb anion is in the Sb^{1-} oxidation state in $CoSb_3$. In the absence of a Sb atom in $CoSb_3$, a single electron is unpaired. Due to the large lattice distortion [Fig. 2(d)], the Sb 5*p*-like defect states become deep inside the band gap, as shown in Fig. 4(d). We find the V_{Sb} can be a deep hole trap of V_{Sb}^{1+}, and also a deep electron trap of V_{Sb}^{1-} or V_{Sb}^{3-}. The (1+/0), (0/1−), and (1−/3−) transition levels are calculated to be E_v+125, 149, 199 meV, respectively. The defect-related states of the Co_i, V_{Co}, Sb_i, and V_{Sb} are schematically drawn in Fig. 5 for easy view.

D. Co-interstitial pair

In Co-rich $CoSb_3$, the formation energy of Co_i is very low as described above. The equilibrium concentration of Co_i is estimated from $[Co_i]=N_0\exp(-\Omega_f/kT_g)$, where N_0 is the number of available sites for Co_i's, Ω_f is the formation energy of Co_i, and T_g is the growth temperature. The N_0 is 3.385×10^{22} cm^{-3} in $CoSb_3$, which is calculated from the theoretical lattice constant of 8.917 Å and the 24 Co_i available sites in the conventional cell. The experimental growth temperature varies from about 900 to 1500 K.[5,6,8–10,13] When the growth temperature is 1200 K, the $[Co_i]$ is calculated to be about 1.5×10^{19} cm^{-3}. At the growth temperature of 1400 K, the $[Co_i]$ is as rich as 4.5×10^{19} cm^{-3}. In such a high concentration of Co_i in Co-rich $CoSb_3$, we examined the possibility of Co_i-pair formation. We consider six different Co_i-pair structures shown in Fig. 6. Three of them are consisted of two sevenfold Co_i's [Figs. 6(a)–6(c)], and two of them are consisted of sevenfold and sixfold Co_i's [Figs. 6(d) and 6(e)]. One is consisted of two sixfold Co_i's [Fig. 6(f)]. Among the Co_i-pairs, the closest pair between two sevenfold Co_i's is found to be the most stable, which is shown in Fig. 6(a). In this pair structure, each Co_i has the coordination number of eight with the additional Co_i-Co_i bond. The other sevenfold Co_i-pairs are higher in energy by about 0.02–0.10 eV [Figs. 6(b) and 6(c)]. Although the energy difference is not large, the additional Co_i-Co_i bond formation in the pair structure shown in Fig. 6(a) is considered to make the structure be the most stable. When the sixfold Co_i is involved in the pair structure, the energies are found to be higher by about 0.13–0.30 eV in the sevenfold and sixfold Co_i-pairs [Figs. 6(d) and 6(e)] and 0.60 eV in the sixfold and sixfold Co_i-pair [Fig. 6(f)].

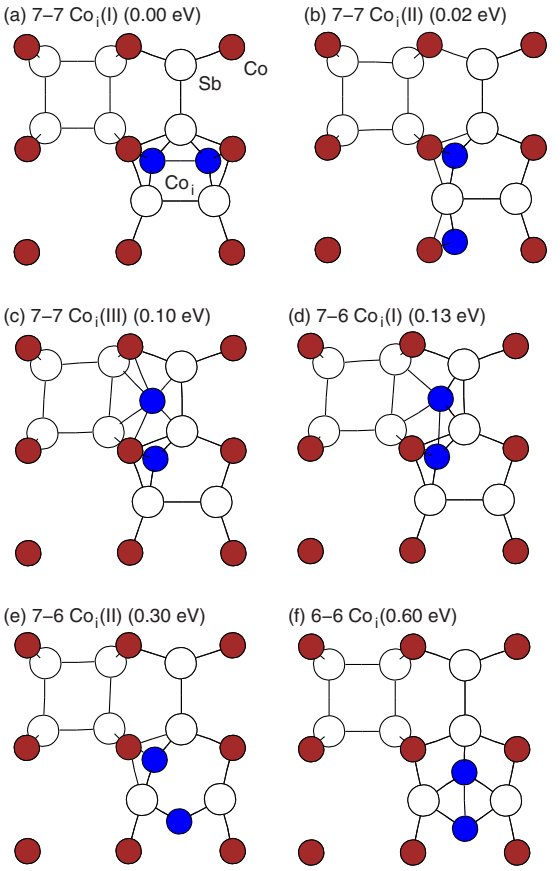

FIG. 6. (Color online). Relaxed atomic structures of Co_i-pairs consisted of [(a), (b), and (c)] two sevenfold Co_i's (7-7 Co_i), [(d) and (e)] sevenfold and sixfold Co_i's (7-6 Co_i), and (f) two sixfold Co_i's (6-6 Co_i). The relative energies relative to the most stable (a) 7-7 Co_i configuration are indicated. The small and large circles are Co and Sb atoms, respectively. The Co_i's are indicated by the blue (dark gray) color.

The formation energy of the most stable Co_i-pair is plotted as a function of the Fermi level, in compared with that of the isolated two Co_i's, in Fig. 7(a). The Co_i-pair is found to be more stable than two isolated Co_i's, especially when the Fermi level is at the lower part of the band gap. The binding energy depends on the Fermi level. When the Fermi level is at the VBM in *p*-type $CoSb_3$, it is 0.47 eV. When the Fermi level is near the CBM in *n*-type $CoSb_3$, it is found to be negligible.

By pairing of the Co_i's, the 3*d*-like defect states of Co_i's are mixed and those levels are altered. The calculated local density of states of the Co_i-pair is drawn in Fig. 7(b), which can be compared with that of the isolated Co_i shown in Fig. 4(a). We find that the singly occupied highest 3*d*-like state of Co_i becomes deeper inside the band gap by the pairing and fully unoccupied. Two of the resonant occupied 3*d*-like states of Co_i are found to be emerged inside the band gap with fully occupied. The occupied 3*d*-like gap states are

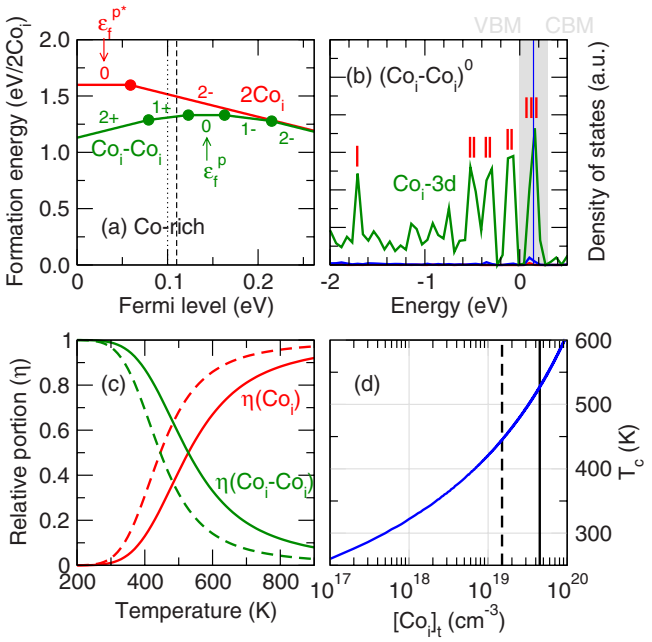

FIG. 7. (Color online). (a) Calculated formation energies of Co_i-pair and two isolated Co_i's plotted as a function of the Fermi level in the Co-rich limit of $CoSb_3$. (b) Calculated projected local density of states of Co_i-pair in the neutral charge state. (c) Relative portions of Co_i [$\eta(Co_i)$], and Co_i-pair [$\eta(Co_i$-$Co_i)$] as a function of temperature, when $[Co_i]_t$ is 4.5×10^{19} cm^{-3} (solid) and 1.5×10^{19} cm^{-3} (dashed). (d) Calculated T_c as a function of $[Co_i]_t$.

found to act as donor levels. Thus, the Co_i-pairs have both the donor characters in the $(Co_i$-$Co_i)^{1+}$ and $(Co_i$-$Co_i)^{2+}$ states, and the acceptor characters in the $(Co_i$-$Co_i)^{1-}$ and $(Co_i$-$Co_i)^{2-}$ states, as can be seen in Fig. 7(a). When the Co_i pairs are dominant in Co-rich $CoSb_3$, the Fermi level is expected to be pinned between the $(1+/0)$ and $(0/1-)$ transition levels, which are E_v+123 meV and E_v+163 meV, respectively, as indicated by ε_f^p in Fig. 7(a). The pinning level, ε_f^p, is found to be higher than the intrinsic Fermi level, ε_f^0, of $CoSb_3$. The formation of the Co_i-pairs as a dominant defect species therefore can higher the Fermi level above the ε_f^0 of $CoSb_3$, resulting in the n-type doping in Co-rich $CoSb_3$.

E. Decomposition of Co_i-pairs

The weak binding energy of Co_i-pairs implies that, at high enough temperature, the Co_i-pairs can be decomposed into the isolated Co_i's. We estimated the decomposition temperature (T_c) of Co_i-pairs in Co-rich $CoSb_3$, which can correspond to the transition temperature of the majority carrier types. The decomposing reaction of $(Co_i$-$Co_i)\rightarrow 2Co_i$ is considered. During the decomposition process, the pinning Fermi level should be changed from the high ε_f^p in the paired state to the low ε_f^{p*} in the isolated state [see ε_f^p and ε_f^{p*} in Fig. 7(a)] by the change in the dominant defect species. Thus, we consider the reaction between the neutral species, i.e., $(Co_i$-$Co_i)^0\rightarrow 2Co_i^0$, which is an endothermic reaction with the formation enthalpy change (ΔH) of 0.27 eV. To consider the temperature effect, we calculate the Gibbs free energy change (ΔG) as $\Delta G=\Delta H-T\Delta S$ including the entropy change (ΔS). The entropy change between the reactants and the products is estimated by the configurational entropy change, $\Delta S=k\{\ln[N(N-1)]-\ln(2N)\}$, where N is the number of available sites per a single Co_i in a fixed concentration of Co_i's. By pairing, the number of available sites per a Co_i-pair becomes $2N$. The total number of available sites (N_0) is 3.385×10^{22} cm^{-3}. If $[Co_i]_t$, which is the total concentration of Co_i including the isolated and paired Co_i's ($[Co_i]+2[Co_i$-$Co_i]$), is 10^{19} cm^{-3}, the N is $N_0/[Co_i]_t=3385$.

There can be also vibrational enthalpy and entropy changes between the isolated and paired states. However, their contributions are found to be very small, only an order of $\Delta H\sim37$ meV and $T\Delta S\sim96$ meV at 600 K, because the additional Co_i-Co_i bond in the paired state has a weak vibrational frequency; the calculated value for the Co_i-Co_i stretch mode is 275 cm^{-1}. The zero point energy is only about 17 meV. The $T\Delta S$ by the configuration entropy change is 0.384 eV at 600 K. Without the vibrational contributions, the estimated T_c can be an upper bound.

The calculated relative portions of Co_i [$\eta(Co_i)$] and Co_i-pair [$\eta(Co_i$-$Co_i)$] with respect to the $[Co_i]_t$ are drawn in Fig. 7(c). For $[Co_i]_t=4.5\times10^{19}$ cm^{-3}, at low temperature below 530 K, the Co_i-pair is found to be dominant, and the isolated Co_i becomes dominant against the Co_i-pair above 530 K. The T_c of 530 K is close to the experimental values of 500–600 K.[5,7–10] In Fig. 7(d), we plot the calculated T_c as a function of $[Co_i]_t$. When $[Co_i]_t$ is 1.5×10^{19} cm^{-3}, the T_c is found to be about 450 K [Figs. 7(c) and 7(d)]. Such a decreased T_c has been also observed in experiment as increasing the excess Sb, i.e., decreasing the Sb deficiency.[10]

IV. CONCLUSION

In conclusion, in Sb-rich and Co-rich $CoSb_3$, V_{Co} and Co_i, respectively, are found to be the dominant native point-defects. Both the V_{Co} and Co_i are acceptorlike defects. The Co_i's can be paired and the pair is found to be a donorlike defect. In Sb-rich $CoSb_3$, the V_{Co} can lead to the p-type doping. In Co-rich $CoSb_3$, at low temperature, where the Co_i pairs are not decomposed, the Co_i-pairs can give the n-type doping. At high temperature, the Co_i-pairs are decomposed into the isolated Co_i's, and the Co-rich $CoSb_3$ can be p-type doped.

ACKNOWLEDGMENT

This work was supported by Nano R&D program through the National Research Foundation of Korea funded by the Ministry of Education, Science, and Technology (Grant No. 2009-0082489).

*yongsung.kim@kriss.re.kr

[1] B. C. Sales, D. Mandrus, and R. K. Williams, Science **272**, 1325 (1996).
[2] G. S. Nolas, M. Kaeser, R. T. Littleton IV, and T. M. Tritt, Appl. Phys. Lett. **77**, 1855 (2000).
[3] M. S. Toprak, C. Stiewe, D. Platzek, S. Williams, L. Bertini, E. Müller, C. Gatti, Y. Zhang, M. Rowe, and M. Muhammed, Adv. Funct. Mater. **14**, 1189 (2004).
[4] G. K. H. Madsen and D. J. Singh, Comput. Phys. Commun. **175**, 67 (2006).
[5] J. W. Sharp, E. C. Jones, R. K. Williams, P. M. Martin, and B. C. Sales, J. Appl. Phys. **78**, 1013 (1995).
[6] Y. Kawaharada, K. Kurosaki, M. Uno, and S. Yamanaka, J. Alloys Compd. **315**, 193 (2001).
[7] V. L. Kuznetsov, L. A. Kuznetsova, and D. M. Rowe, J. Phys.: Condens. Matter **15**, 5035 (2003).
[8] K. T. Wojciechowski, J. Tobola, and J. Leszczyński, J. Alloys Compd. **361**, 19 (2003).
[9] W.-S. Liu, B.-P. Zhang, J.-F. Li, and L.-D. Zhao, J. Phys. D **40**, 566 (2007).
[10] W.-S. Liu, B.-P. Zhang, J.-F. Li, and L.-D. Zhao, J. Phys. D **40**, 6784 (2007).
[11] D. T. Morelli, T. Caillat, J.-P. Fleurial, A. Borshchevsky, J. Vandersande, B. Chen, and C. Uher, Phys. Rev. B **51**, 9622 (1995).
[12] E. Arushanov, K. Fess, W. Kaefer, Ch. Kloc, and E. Bucher, Phys. Rev. B **56**, 1911 (1997).
[13] Z. Zhou, C. Uher, A. Jewell, and T. Caillat, Phys. Rev. B **71**, 235209 (2005).
[14] T. Caillat, A. Borshchevsky, and J.-P. Fleurial, J. Appl. Phys. **80**, 4442 (1996).
[15] D. J. Singh and W. E. Pickett, Phys. Rev. B **50**, 11235 (1994).
[16] J. O. Sofo and G. D. Mahan, Phys. Rev. B **58**, 15620 (1998).
[17] K. Koga, K. Akai, K. Oshiro, and M. Matsuura, Phys. Rev. B **71**, 155119 (2005).
[18] P. Ghosez and M. Veithen, J. Phys.: Condens. Matter **19**, 096002 (2007).
[19] G. Kresse and D. Joubert, Phys. Rev. B **59**, 1758 (1999).
[20] P. E. Blöchl, Phys. Rev. B **50**, 17953 (1994).
[21] D. M. Ceperley and B. J. Alder, Phys. Rev. Lett. **45**, 566 (1980).
[22] Th. Schmidt, G. Kliche, and H. D. Lutz, Acta Crystallogr., Sect. C: Cryst. Struct. Commun. **43**, 1678 (1987).
[23] L. D. Dudkin and N. K. Abrikosov, Zh. Neorg. Khim. **1**, 2096 (1956); Russ. J. Inorg. Chem. **1**, 169 (1956).
[24] J. E. Northrup and S. B. Zhang, Phys. Rev. B **50**, 4962 (1994).
[25] Y.-S. Kim and C. H. Park, Phys. Rev. Lett. **102**, 086403 (2009).
[26] H. Anno, K. Matsubara, T. Caillat, and J.-P. Fleurial, Phys. Rev. B **62**, 10737 (2000).
[27] I. Barin *et al.*, *Thermochemical Data of Pure Substances* (Wiley-VCH, New York, 1992).
[28] A. F. Kohan, G. Ceder, D. Morgan, and Chris G. Van de Walle, Phys. Rev. B **61**, 15019 (2000).
[29] S. B. Zhang, S.-H. Wei, and A. Zunger, Phys. Rev. B **63**, 075205 (2001).
[30] P. Erhart, A. Klein, and K. Albe, Phys. Rev. B **72**, 085213 (2005).
[31] A. Janotti and C. G. Van de Walle, Phys. Rev. B **76**, 165202 (2007).
[32] G. Makov and M. C. Payne, Phys. Rev. B **51**, 4014 (1995).
[33] G. Kliche and H. D. Lutz, Infrared Phys. **24**, 171 (1984).
[34] D. Jung, M.-H. Whangbo, and S. Alvarez, Inorg. Chem. **29**, 2252 (1990).